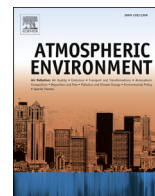




Contents lists available at ScienceDirect

## Atmospheric Environment

journal homepage: [www.elsevier.com/locate/atmosenv](http://www.elsevier.com/locate/atmosenv)

## Characteristics and applications of size-segregated biomass burning tracers in China's Pearl River Delta region



Zhisheng Zhang<sup>a, b</sup>, Jian Gao<sup>b, \*</sup>, Guenter Engling<sup>c, d, \*\*</sup>, Jun Tao<sup>a</sup>, Fahe Chai<sup>b</sup>,  
Leiming Zhang<sup>e</sup>, Renjian Zhang<sup>f</sup>, Xuefang Sang<sup>g, 1</sup>, Chuen-yu Chan<sup>g, h</sup>, Zejian Lin<sup>a</sup>,  
Junji Cao<sup>h</sup>

<sup>a</sup> South China Institute of Environmental Sciences, Ministry of Environmental Protection, Guangzhou, China

<sup>b</sup> Chinese Research Academy of Environmental Sciences, Beijing, China

<sup>c</sup> Department of Biomedical Engineering and Environmental Sciences, National Tsing Hua University, Hsinchu, Taiwan

<sup>d</sup> Division of Atmospheric Sciences, Desert Research Institute, Reno, NV, USA

<sup>e</sup> Air Quality Research Division, Science Technology Branch, Environment Canada, Toronto, Canada

<sup>f</sup> RCE-TEA, Institute of Atmospheric Physics, Chinese Academy of Sciences, Beijing, China

<sup>g</sup> Sun Yat-sen University, Guangzhou, China

<sup>h</sup> Key Laboratory of Aerosol, SKLLQG, Institute of Earth Environment, Chinese Academy of Sciences, Xi'an, China

### H I G H L I G H T S

- First report of size distributions of biomass burning tracers in the PRD.
- Origins of biomass burning aerosols were identified using multiple tracer method.
- Biomass smoke contributed significantly to ambient aerosol in the PRD region.

### A R T I C L E I N F O

#### Article history:

Received 29 June 2014

Received in revised form

2 December 2014

Accepted 3 December 2014

Available online 4 December 2014

#### Keywords:

Biomass combustion

Size distribution

Anhydrosugars

Potassium

Source-receptor study

### A B S T R A C T

Biomass burning activities in China are ubiquitous and the resulting smoke emissions may pose considerable threats to human health and the environment. In the present study, size-segregated biomass burning tracers, including anhydrosugars (levoglucosan (LG) and mannosan (MN)) and non-sea-salt potassium (nss-K<sup>+</sup>), were determined at an urban and a suburban site in the Pearl River Delta (PRD) region. The size distributions of biomass burning tracers were generally characterized by a unimodal pattern peaking in the particle size range of 0.44–1.0 μm, except for MN during the wet season, for which a bimodal pattern (one in fine and one in coarse mode) was observed. These observed biomass burning tracers in the PRD region shifted towards larger particle sizes compared to the typical size distributions of fresh biomass smoke particles. Elevated biomass burning tracers were observed during the dry season when biomass burning activities were intensive and meteorological conditions favored the transport of biomass smoke particles from the rural areas in the PRD and neighboring areas to the sampling sites. The fine mode biomass burning tracers significantly correlated with each other, confirming their common sources. Rather high ΔLG/ΔMN ratios were observed at both sites, indicating limited influence from softwood combustion. High Δnss-K<sup>+</sup>/ΔLG ratios further suggested that biomass burning aerosols in the PRD were predominately associated with burning of crop residues. Using a simplified receptor-oriented approach with an emission factor of 0.075 (LG/TC) obtained from several chamber studies, average contributions of biomass burning emissions to total carbon in fine particles were estimated to be 23% and 16% at the urban and suburban site, respectively, during the dry season. In

\* Corresponding author. No.8 Dayangfang, Anwai Beiyuan, Chaoyang district, Beijing, China.

\*\* Corresponding author. No. 101, Section 2, Kuang-Fu Road, Hsinchu, Taiwan.

E-mail addresses: [gaojian@craes.org.cn](mailto:gaojian@craes.org.cn) (J. Gao), [guenter@mx.nthu.edu.tw](mailto:guenter@mx.nthu.edu.tw) (G. Engling).

<sup>1</sup> Now working at IEK-8: Troposphäre, Forschungszentrum Jülich, Jülich, Germany.

contrast, the relative contributions to total carbon were lower than 8% at both sites during the wet season.

© 2014 Elsevier Ltd. All rights reserved.

## 1. Introduction

Atmospheric particulate matter (PM) exerts significant influence on cloud formation, radiation budget and air quality, and ultimately affects global climate and human health (Pöschl, 2005; Seinfeld and Pandis, 2006). Recently, there has been growing public concern about the high PM levels and reduced visibility in Asia, especially in China. Facing severe air pollution problems, the Chinese government has recently revised the national ambient air quality standard, which will be implemented countrywide in 2016. This is the first standard in China that sets a critical level for PM<sub>2.5</sub> (particulate matter with aerodynamic diameters smaller than 2.5 μm). Therefore, an understanding of source contributions to PM<sub>2.5</sub> and its major components in various regions of China is urgently required to provide scientific evidence for establishing pollutant control policies and strategies.

Inorganic ions and carbonaceous species are major chemical components of PM (Jimenez et al., 2009). The dominant inorganic ions include sulfate, nitrate, ammonium and basic cations. Their sources and formation mechanisms are generally well understood (Alexander et al., 2005; Michalski et al., 2003; Zhang et al., 2008a). Strict emission control policies have been established in China for controlling the gaseous precursors forming sulfate and nitrate. However, knowledge of source contributions to carbonaceous species is still limited. An early study on global emission inventories suggested that biomass burning was the largest source of primary organic carbon (POC) and elemental carbon (EC) (Bond et al., 2004). About 31 TgC yr<sup>-1</sup> POC and 5.0 TgC yr<sup>-1</sup> EC were produced from biomass burning processes, accounting for 93% and 62% of the total global EC and POC emissions, respectively. Although biomass burning is a significant source of carbonaceous matter as well as PM<sub>2.5</sub> in general, little attention has been paid to this source by policy-makers due to the dominant influence of urban and industrial activities on PM<sub>2.5</sub>.

Both source-oriented and receptor-based approaches have been used to quantify biomass burning contributions to PM<sub>2.5</sub> (e.g., Zhang et al., 2010a). Source-oriented methods rely on emission inventories and meteorological parameters to estimate the impact of particular sources. However, large uncertainties exist in the biomass burning activity data, and emission factors also vary greatly under different combustion conditions (Tian et al., 2008). Over the past decade, receptor-oriented methods have become the primary impact assessment tool for biomass burning, especially studies based on the measurements of source-specific tracers (Ho et al., 2014; Zhang et al., 2013a, 2010a; Zheng et al., 2002). The most commonly used biomass burning tracers are anhydrosugars (i.e., LG, MN and galactosan), of which LG is the single most abundant component in biomass burning smoke. Anhydrosugars are the pyrolysis products of cellulose and hemicellulose and have not been found in other types of combustion processes (Simoneit, 2002). Although the emission factors of anhydrosugars have been found to vary significantly with biomass types and burning conditions (Sullivan et al., 2008), they have been used extensively to estimate biomass burning contributions to PM<sub>2.5</sub> and carbonaceous species masses (Harrison et al., 2012; Zhang et al., 2008b, 2010b). Water-soluble potassium is also regarded as a reliable tracer for biomass burning, although corrections are needed due to the

contributions from other potential sources such as soil and sea-salt (Duan et al., 2004).

The Pearl River Delta (PRD) region is one of the most developed areas in China and has long been suffering of serious PM pollution (Chan and Yao, 2008). An increasing demand for cleaner air from the public drives the government and the scientific community to better understand PM sources, formation mechanisms and control strategies. The PRD region also plays a leading role in the establishment of China's air pollution control and prevention policies, and the experience gained in this region will benefit other parts of the country. From the emission inventory studies for the PRD region, biomass burning has been recently identified as an important source of PM<sub>2.5</sub> in the PRD region, producing 0.03 Tg or 15% of the total PM<sub>2.5</sub> (He et al., 2011; Zheng et al., 2009). As suggested by Zhang et al. (2010b), biomass burning aerosols generated in the rural areas of the PRD and Guangdong province can be transported to the urban areas resulting in serious biomass burning episodic events. Biomass burning activities are common in the surrounding areas of the PRD region, although there is still very limited knowledge regarding the major type of biomass burning aerosols influencing the PRD region and other parts of China.

The purpose of the present study is, therefore, to identify the sources of biomass burning aerosols and quantify the contributions of biomass burning activities to the total carbon (TC) content in PM<sub>2.5</sub> in the PRD region. This is achieved through measurement of multiple biomass burning tracers in size-segregated aerosol samples at an urban and a suburban site within the PRD during typical dry and wet seasons. Knowledge gained from this study will also benefit other regions of China, where biomass burning activities are common practice, e.g., in the region of the Sichuan basin and North China (Tao et al., 2013).

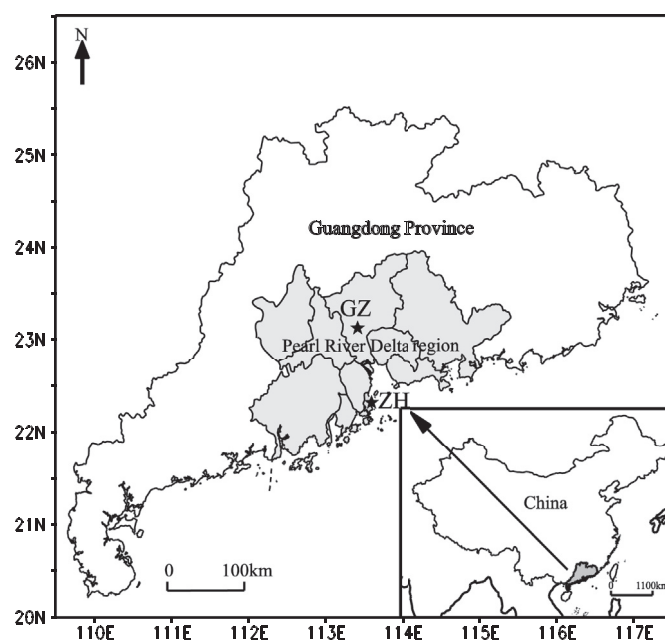


Fig. 1. Location of the sampling sites.

## 2. Experimental

### 2.1. Sampling site description

Two sites, one urban and one suburban, were selected for aerosol sampling. The urban site (GZ, 23.12°N, 113.36°E, Fig. 1) is located inside a megacity, Guangzhou, the capital and the largest city of Guangdong province with a population exceeding 12 million. The sampling instrument was set on the roof of a fourteen-floor building (~50 m above ground) at the South China Institute of Environmental Sciences (SCIES). The sampling site is surrounded by many low residential/commercial buildings without any obvious industrial activities within 5 km, although with a main traffic road 200 m away (Tao et al., 2012). It is believed to represent a typical urban environment in the PRD region.

The suburban site (ZH, 22.34°N, 113.58°E) is located in a suburban area of Zhuhai, a city with a population of around 1.5 million. Zhuhai borders Macao to the south and lies on the southwestern tip of the PRD. The city was built as a garden style city and is recognized internationally as an environment-friendly city with good air quality throughout most of the year. Aerosol samples were collected on the roof of a library building (~60 m above ground) at the Zhuhai campus of Sun Yat-sen University. This site is surrounded by small hills at three sides and faces the South China Sea at one side (with a distance of around 700 m to the ocean). It is regarded as an ideal location in the PRD region for the measurement of background levels of PM<sub>2.5</sub> in terms of biomass burning source impact. The distance between the two monitoring sites is around 90 km.

### 2.2. Aerosol collection

Size-segregated aerosol samples were collected at both sites from May to June and from November to December of 2010 (Table 1). The former period corresponds to the typical wet season, while the latter one represents the dry season in the PRD region. Two six-stage high flow impactors (Model 131, MSP Corporation, Shoreview, MN, USA) with cut-point diameters of 10, 2.5, 1.4, 1.0, 0.44 and 0.25 μm were employed. The samplers were operated at 100 L min<sup>-1</sup> for approximately 24 h, loaded with pre-baked quartz fiber filters (Pall Corporation, NY, USA) to collect one set of samples. Static field blanks were collected by mounting filters on each stage for 5–10 min without turning the pump on. The collected samples and blanks were stored at <4 °C before chemical analysis.

### 2.3. Chemical analyses

A portion of each quartz filter (1.5 cm<sup>2</sup>) was cut and used to determine the carbonaceous species using a thermal/optical transmittance aerosol carbon analyzer (Sunset Laboratory, OR, USA). The first stage of carbon analysis, in an inert helium atmosphere, consisted of four temperature steps: 250 °C (60 s), 500 °C (60 s), 650 °C (60 s), and 850 °C (120 s). In the second stage, the analysis was conducted under an environment of 2% O<sub>2</sub>/98% He,

and the temperature was set as: 550 °C (45 s), 625 °C (45 s), 700 °C (45 s), 775 °C (45 s), 850 °C (45 s), and 870 °C (120 s). Due to the non-uniform particle deposition on the filters collected by the cascade impactors, laser correction did not work properly to separate OC and EC based on this protocol. However, this condition did not affect the TC determination (Chow et al., 2001). Blank samples were analyzed according to the same procedures as the ambient samples, and the results of all samples reported here were blank corrected. The limit of detection (LOD) of TC was estimated to be 0.04 μgC m<sup>-3</sup>.

LG and MN, as well as other carbohydrates were determined by high performance anion exchange chromatography with pulsed amperometric detection (HPAEC-PAD), which is a well-established method for poly-hydroxy organic compounds that has been successfully applied for measuring saccharidic tracers in several studies. The detailed analysis procedures can be found in Zhang et al. (2013c). Briefly, 1/4 quartz filter portions were extracted by deionized ultrapure water in pre-baked glass bottles under ultrasonic agitation for 60 min. The filter extracts were filtered through Teflon syringe filters to remove insoluble materials, and were subsequently analyzed on a Dionex ICS-3000 system with a Dionex Carpac MA1 analytical column (250 × 4 mm). The LOD of LG and MN were estimated to be 0.4 ng m<sup>-3</sup> and 0.2 ng m<sup>-3</sup>, respectively, in this study. The anhydrosugar content in all field blanks was lower than the LOD.

Water-soluble potassium as well as other inorganic ions were quantified on a Dionex ICS-3000 ion chromatograph using the same filter extracts. The cations were separated on an Ionpac CS12 analytical column with CG12 guard column using 20 mM methanesulfonic acid as eluent at a flow rate of 1.0 mL min<sup>-1</sup>, while the anions were separated with an Ionpac AS14 analytical and AG14 guard column with a mixture of 4.5 mM Na<sub>2</sub>CO<sub>3</sub> and 1.4 mM NaHCO<sub>3</sub> as eluent at a flow rate of 1.2 mL min<sup>-1</sup>. The LOD of water-soluble potassium was estimated to be 1.5 ng m<sup>-3</sup>. The potassium concentrations presented here were corrected by field blanks and by a sea salt indicator (magnesium), i.e.,  $C_{\text{K}^+}^{\text{corrected}} = C_{\text{K}^+} - 0.159 * C_{\text{Mg}^{2+}}$  (Cheng et al., 2000).

### 2.4. Meteorological data and air mass history analysis

The major meteorological parameters were obtained at both sites using Vaisala Automatic Weather Stations, as detailed in Tao et al. (2014). Table 1 presents the mean daily temperature, pressure, relative humidity and total rainfall throughout the campaign. The wet season was characterized by high relative humidity and intensive rainfall, while the dry season was marked by low relative humidity and no precipitation. To eliminate the scavenging effects on aerosols during precipitation events, it should be noted that, for both seasons, only samples collected on days without or with negligible rain amount were selected for further chemical analysis.

Open burning events were detected by the Moderate-Resolution Imaging Spectroradiometer (MODIS) mounted on NASA's Terra and Aqua satellites to identify outdoor biomass burning activities over South China during the sampling periods. The data set had a

**Table 1**  
Summary of meteorological conditions at the urban and suburban site during the sampling periods.

Site	Season	Sampling period	RH (%)	Temperature (°C)	Rainfall <sup>a</sup> (mm)	Pressure (hPa)	Wind speed (m s <sup>-1</sup> )
Urban	Wet	2010/5/4–2010/6/20	75.5 ± 13	26.4 ± 2.6	507.8	999.4 ± 2.1	1.4 ± 1.2
	Dry	2010/11/12–2010/12/9	48.5 ± 13	21.1 ± 3.0	0	1008.5 ± 2.5	0.5 ± 0.7
Suburb	Wet	2010/5/4–2010/6/20	78.3 ± 6.3	26.2 ± 1.8	365	1000.7 ± 1.6	3.1 ± 1.6
	Dry	2010/11/12–2010/11/28	65.9 ± 4.9	21.1 ± 1.1	0.4	1008.7 ± 2.4	1.9 ± 1.2

<sup>a</sup> Data are presented as the total amount for rainfall during the sampling periods, and as the daily mean ± one standard deviation for the rest of the meteorological parameters.

horizontal resolution of  $1 \times 1 \text{ km}^2$  and is available on NASA's website (<http://earthdata.nasa.gov/data/near-real-time-data/firms>).

To track air masses reaching the PRD region, 72-h backward air mass trajectories were calculated by the HYSPLIT model (available at <http://ready.arl.noaa.gov/HYSPLIT.php>). The FNL (Final Operational Global Analysis) meteorological data were chosen as the input. An altitude of 1500 m above ground level was the starting height of all trajectories. The backward trajectories were computed at 14:00 UTC of each sampling day, corresponding to the midpoint of each 24-h sample collection period.

### 3. Results and discussion

#### 3.1. Size distributions of biomass burning tracers

Particle size is a critical aerosol physical parameter affecting aerosol transport, cloud formation and optical properties; yet it is rarely measured for biomass burning aerosols in field studies. The size distributions of multiple biomass burning tracers are presented in Fig. 2 and their mass concentrations at each particle size range

are listed in Table 2. Generally, the size distributions of biomass burning tracers were characterized by a unimodal pattern peaking in the fine mode ( $0.44\text{--}1 \mu\text{m}$ ). The only exception was observed for MN at the urban site during the wet season, which showed a bimodal pattern, with one mode in fine particles ( $0.44\text{--}1 \mu\text{m}$ ) and another smaller one in coarse particles ( $2.5\text{--}10 \mu\text{m}$ ).

Both LG and  $\text{nss-K}^+$  were found predominately in the size range of  $0.44\text{--}1.0 \mu\text{m}$  in all sample sets. The LG fraction present in this size range accounted for 48.3% and 44.7% of all size fractions on average for the wet and dry season, respectively, at the urban site. The LG fraction in this size range was 51.1% at the suburban site during the dry season. On the other hand, the percentages of the  $\text{nss-K}^+$  mass concentration in this size range were 44.3% and 46.7% during the wet and dry season, respectively, at the urban site, and 41.9% and 48.9%, respectively, at the suburban site. These values were similar to those of LG. MN also showed a similar size distribution pattern to LG and  $\text{nss-K}^+$  during the dry season, but a different pattern at the urban site during the wet season as mentioned above. Note that the size distribution of MN at the suburban site during the wet season was not available due to its low concentrations.

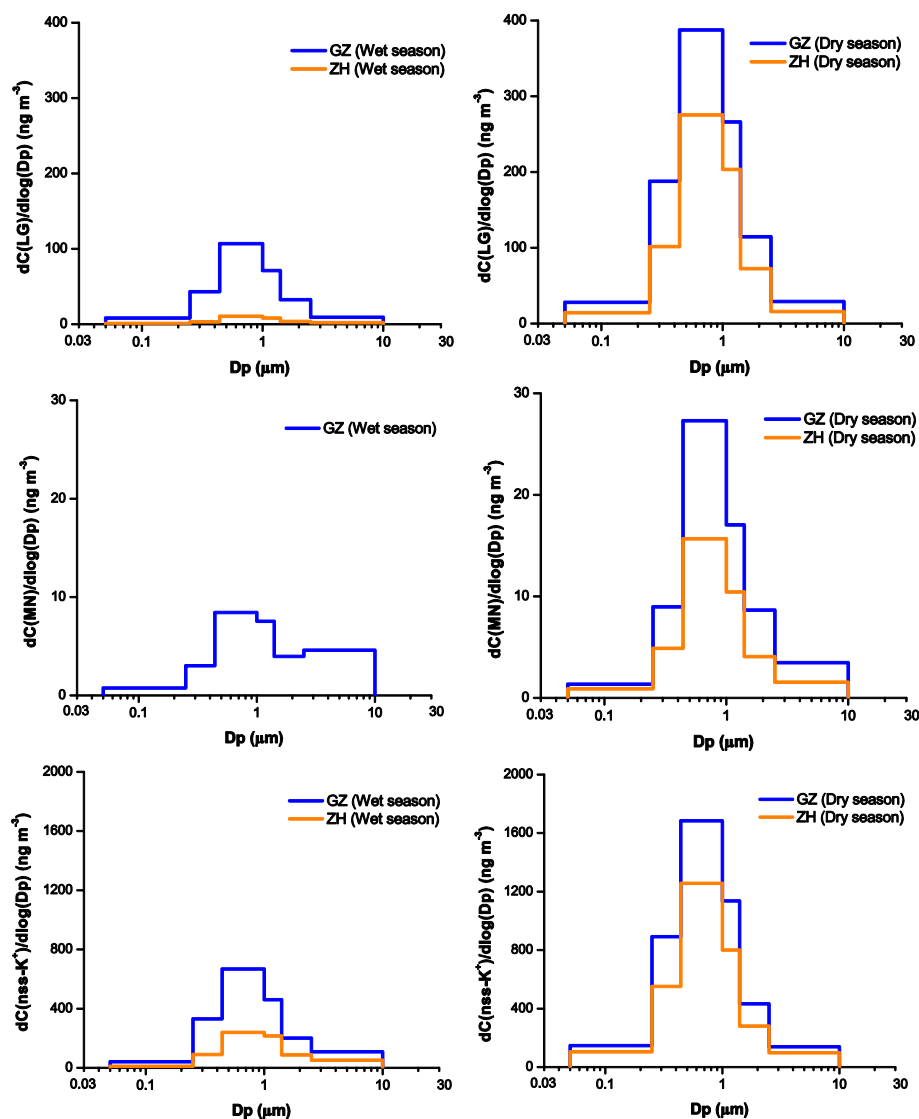


Fig. 2. Size distributions of biomass burning tracers (LG, upper; MN, middle;  $\text{nss-K}^+$ , lower panel) at the urban and suburban site during the wet (left) and dry season (right).

**Table 2**  
Concentrations of size-segregated biomass burning tracers and major particulate component at the urban and suburban site in the PRD region.<sup>a</sup>

	Location	Season	10–2.5 $\mu\text{m}$	2.5–1.4 $\mu\text{m}$	1.4–1.0 $\mu\text{m}$	1.0–0.44 $\mu\text{m}$	0.44–0.25 $\mu\text{m}$	<0.25 $\mu\text{m}$	PM <sub>2.5</sub>
LG (ng m <sup>-3</sup> )	Urban	Wet	5.6 ± 5.3 (10)	8.2 ± 12.3 (10)	10.4 ± 15.5 (10)	38.1 ± 40.9 (10)	10.6 ± 10.5 (10)	5.7 ± 2.6 (10)	73.0 ± 81.1
		Dry	17.5 ± 9.0 (14)	28.9 ± 11.4 (14)	38.9 ± 15.5 (14)	138.2 ± 55.1 (14)	46.1 ± 18.9 (14)	19.7 ± 7.3 (14)	272 ± 103
	Suburb	Wet	1.3 ± 0.9 (4)	1.4 ± 1.0 (5)	2.2 ± 1.8 (4)	3.8 ± 5.3 (8)	1.3 ± 1.1 (4)	1.0 ± 0.4 (6)	7.5 ± 8.7 <sup>b</sup>
		Dry	9.5 ± 5.4 (9)	18.3 ± 13.3 (9)	29.7 ± 22.6 (9)	98.2 ± 67.4 (9)	24.9 ± 16.6 (9)	10.0 ± 5.7 (9)	181 ± 124
MN (ng m <sup>-3</sup> )	Urban	Wet	2.8 ± 2.8 (8)	1.0 ± 1.3 (10)	1.1 ± 1.6 (9)	3.0 ± 3.6 (9)	0.7 ± 0.7 (10)	0.5 ± 0.4 (7)	5.8 ± 7.3
		Dry	2.1 ± 1.1 (14)	2.2 ± 0.9 (14)	2.5 ± 1.1 (14)	9.7 ± 4.2 (14)	2.2 ± 1.2 (13)	0.9 ± 0.4 (9)	17.4 ± 7.1
	Suburb	Wet	L.D. <sup>c</sup>	L.D.	L.D.	1.1 ± 0.2 (2)	L.D.	L.D.	
		Dry	0.9 ± 0.5 (9)	1.0 ± 0.5 (9)	1.5 ± 1.2 (9)	5.6 ± 4.0 (9)	1.2 ± 0.6 (9)	0.6 ± 0.3 (9)	10.0 ± 6.2
nss-K <sup>+</sup> (ng m <sup>-3</sup> )	Urban	Wet	65.0 ± 27.3 (10)	50.6 ± 51.4 (10)	67.3 ± 59.3 (10)	238 ± 149 (10)	81.2 ± 45.3 (10)	28.4 ± 11.9 (10)	465 ± 302
		Dry	83.5 ± 33.3 (14)	109 ± 45.7 (14)	166 ± 58.9 (14)	600 ± 190 (14)	219 ± 63.8 (14)	103 ± 28.1 (14)	1197 ± 356
	Suburb	Wet	31.1 ± 12.2 (8)	22.0 ± 15.7 (8)	31.5 ± 24.5 (8)	85.4 ± 51.5 (8)	22.1 ± 9.2 (8)	7.2 ± 3.3 (8)	168 ± 99.2
		Dry	58.5 ± 24.4 (9)	70.6 ± 34.6 (9)	117 ± 49.5 (9)	448 ± 183 (9)	135 ± 51.6 (9)	73.3 ± 26.3 (9)	844 ± 325
TC ( $\mu\text{gC m}^{-3}$ )	Urban	Wet	2.9 ± 1.6 (10)	1.1 ± 0.6 (10)	1.0 ± 0.6 (10)	3.3 ± 2.2 (10)	2.4 ± 1.4 (10)	2.7 ± 0.8 (10)	10.6 ± 5.6
		Dry	3.1 ± 1.5 (14)	1.8 ± 0.7 (14)	1.9 ± 0.6 (14)	5.7 ± 2.1 (14)	3.2 ± 1.2 (14)	3.2 ± 0.9 (14)	15.7 ± 5.3
	Suburb	Wet	0.8 ± 0.5 (8)	0.4 ± 0.2 (8)	0.4 ± 0.3 (8)	1.2 ± 0.9 (8)	0.8 ± 0.5 (8)	1.7 ± 0.6 (8)	4.5 ± 2.4
		Dry	1.8 ± 0.8 (9)	1.4 ± 0.6 (9)	1.8 ± 0.7 (9)	5.5 ± 1.8 (9)	2.8 ± 0.9 (9)	2.5 ± 0.4 (9)	14.0 ± 4.2
NO <sub>3</sub> <sup>-</sup> ( $\mu\text{g m}^{-3}$ )	Urban	Wet	3.67 ± 1.41 (10)	1.17 ± 0.87 (10)	0.86 ± 0.83 (10)	2.28 ± 2.01 (10)	0.41 ± 0.30 (10)	0.26 ± 0.15 (10)	4.98 ± 4.04
		Dry	3.29 ± 2.01 (14)	1.05 ± 0.59 (14)	0.86 ± 0.63 (14)	2.82 ± 2.08 (14)	0.80 ± 0.52 (14)	0.48 ± 0.26 (14)	6.00 ± 3.91
	Suburb	Wet	2.04 ± 0.60 (8)	0.41 ± 0.24 (8)	0.15 ± 0.16 (8)	0.26 ± 0.44 (8)	0.04 ± 0.04 (7)	0.04 ± 0.04 (8)	0.90 ± 0.85
		Dry	3.93 ± 2.59 (9)	1.23 ± 0.43 (9)	1.03 ± 0.50 (9)	2.98 ± 1.58 (9)	0.68 ± 0.33 (9)	0.37 ± 0.12 (9)	6.28 ± 2.80
SO <sub>4</sub> <sup>2-</sup> ( $\mu\text{g m}^{-3}$ )	Urban	Wet	1.60 ± 0.79 (10)	1.62 ± 0.15 (10)	2.02 ± 1.25 (10)	5.76 ± 2.43 (10)	1.51 ± 0.60 (10)	0.75 ± 0.32 (10)	11.65 ± 5.23
		Dry	1.25 ± 0.36 (14)	1.75 ± 0.67 (14)	2.47 ± 1.10 (14)	7.68 ± 2.67 (14)	2.19 ± 0.61 (14)	1.09 ± 0.32 (14)	11.52 ± 4.86
	Suburb	Wet	0.72 ± 0.19 (8)	1.00 ± 0.54 (8)	1.49 ± 0.73 (8)	4.74 ± 1.70 (8)	1.19 ± 0.28 (8)	0.41 ± 0.18 (8)	8.82 ± 3.25
		Dry	1.21 ± 356 (9)	1.77 ± 962 (9)	2.80 ± 1.50 (9)	7.75 ± 2.40 (9)	2.04 ± 0.43 (9)	0.81 ± 0.18 (9)	15.17 ± 5.02
NH <sub>4</sub> <sup>+</sup> ( $\mu\text{g m}^{-3}$ )	Urban	Wet	0.38 ± 0.30 (10)	0.68 ± 0.71 (10)	0.89 ± 0.66 (10)	2.41 ± 1.26 (10)	0.65 ± 0.35 (10)	0.32 ± 0.24 (10)	4.94 ± 2.87
		Dry	0.45 ± 0.29 (14)	0.72 ± 0.28 (14)	1.07 ± 0.43 (14)	3.17 ± 1.09 (14)	1.00 ± 0.29 (14)	0.39 ± 0.22 (14)	6.35 ± 2.08
	Suburb	Wet	0.14 ± 0.11 (8)	0.29 ± 0.23 (8)	0.53 ± 0.29 (8)	1.57 ± 0.60 (8)	0.45 ± 0.13 (8)	0.14 ± 0.052 (8)	2.97 ± 1.23
		Dry	0.41 ± 0.25 (9)	0.61 ± 0.36 (9)	0.99 ± 0.52 (9)	3.06 ± 1.14 (9)	0.73 ± 0.22 (9)	0.34 ± 0.11 (9)	5.73 ± 2.17

<sup>a</sup> Date are presented as mean ± one standard deviation, and the values in brackets are the sample numbers above LOD.

<sup>b</sup> Data below LOD are replaced by half of the LOD values, when adding up to calculate the amount in PM<sub>2.5</sub>.

<sup>c</sup> L.D. represents values lower than LOD.

Comparing the size distributions shown in Table 2 with those observed directly in source emissions, it was found that biomass burning tracers from combustion of several crop residues and fuel wood in South China (shown in Table S1) (Sang, 2012) had larger mass fractions in small particles (e.g., <0.44  $\mu\text{m}$ ) than those observed at the urban and suburban site in this study. This suggests

that smoke particles have a tendency of shifting towards larger particle sizes from the combustion source to downwind receptor sites (i.e., monitoring stations). This trend is in agreement with previously reported findings (e.g., Herckes et al., 2006), which ascribed it to smoke particle aging or hygroscopic growth during transport and transformation processes.

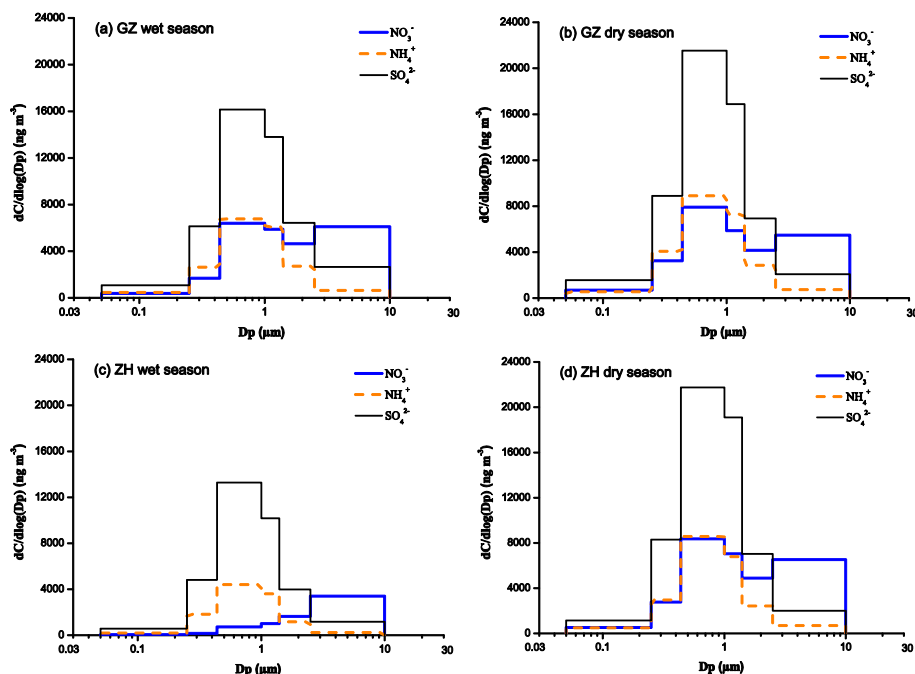


Fig. 3. Size distributions of secondary inorganic aerosol species (SO<sub>4</sub><sup>2-</sup>, NO<sub>3</sub><sup>-</sup> and NH<sub>4</sub><sup>+</sup>).

The shifting to larger sizes for biomass burning aerosols may also be caused by formation of secondary aerosol species and association with the biomass burning aerosols. As shown in Table 2 and Fig. 3, concentrations of secondary inorganic ions (especially sulfate and ammonium) peaked in the accumulation mode, similar to those of biomass burning tracers. The size distributions of biomass burning aerosols seemed to be shifted when mixed with pollution plumes containing substantial amounts of secondary inorganic aerosol precursors (i.e.,  $\text{SO}_2$  and  $\text{NO}_x$ ) derived from urban and industrial activities. Thus, biomass burning aerosols can readily be transported over long distances due to long residence times of accumulation mode aerosols and subsequently impact regional air quality.

Biomass burning smoke apparently also affected other aerosol particle components and their size distributions in the PRD region. Water-soluble chloride salts are usually associated with sea-salt particles, which are exclusively present in the coarse mode. However, a significant amount of chloride was found in fine particles during the dry season. In particular, the chloride content in  $\text{PM}_{2.5}$  at the suburban site was nearly 5 times higher during the dry season than that during the wet season (Table S2). Moreover, the size distribution of chloride at the urban site showed one peak in the fine mode during the dry season (Fig. 4). Earlier studies suggested that biomass burning could be a significant source for atmospheric chloride and chloride-containing compounds (Engling et al., 2009; Lobert et al., 1999). For example, Engling et al. (2009) found that potassium, chloride and ammonium were the most abundant inorganic ions in  $\text{PM}_{2.5}$  measured in rice straw burning smoke. The build-up of fine chloride concentrations during the dry season might be partially attributed to the increase of biomass burning contributions as further discussed below.

### 3.2. Seasonal and spatial variations of tracer levels

The ambient concentrations of the biomass burning tracers in different seasons at both sampling sites are summarized in Table 2. The biomass burning tracers presented a consistent seasonal

pattern with elevated concentrations during the dry season. For example, the average LG concentration in  $\text{PM}_{2.5}$  at the urban site was  $272 \text{ ng m}^{-3}$  during the dry season, which was 3.7 times of that during the wet season ( $73 \text{ ng m}^{-3}$ ). The LG concentration at the suburban site was remarkably higher (by 23 times) during the dry season compared to the wet season. Apparently, both sites received enhanced influence of biomass burning aerosols during the dry season compared to the wet season.

Because commercial energy sources (Such as LPG, biogas and coal) are increasingly available in rural areas of China, large amounts of crop residues are discarded in the field. It is a common practice for field burning of crop residues, especially in economically developed areas of China. It was estimated that over 30% of rice straw is burned directly on fields in Guangdong and Fujian provinces (Cao et al., 2008). Open biomass burning activities in South China were much stronger during the harvest season (coinciding with the dry season here), as seen from MODIS fire counts (Fig. 5), which was consistent with the observed elevated biomass burning tracers in the PRD region.

During the wet season, the predominant pathway of air masses reaching the sampling sites was via the South China Sea, as revealed by the backward trajectory analysis (Fig. 6), under the influence of the East Asian summer monsoon. This was also supported by the fact that significant amounts of sea-salt components ( $\text{Na}^+$ ,  $\text{Cl}^-$  and  $\text{Mg}^{2+}$ ) were found in coarse mode particles at both sampling sites during the wet season (Fig. 4). The air masses with maritime origin brought in relatively clean air to the South China as well as intensive rainfall that could efficiently scavenge atmospheric pollutants. Moreover, fewer biomass burning activities were observed during this period (Fig. 5). Consequently, the influence of biomass burning on ambient atmospheric pollutants was low during the wet season.

On the other hand, a large amount of crop residues are produced during the dry season, which coincides with the autumn harvest period (usually from October to late November) in South China. The air masses of continental origins likely carried the biomass burning aerosols to the PRD region (Fig. 6). Furthermore, the continental air masses were characterized by dry conditions and negligible rainfall.

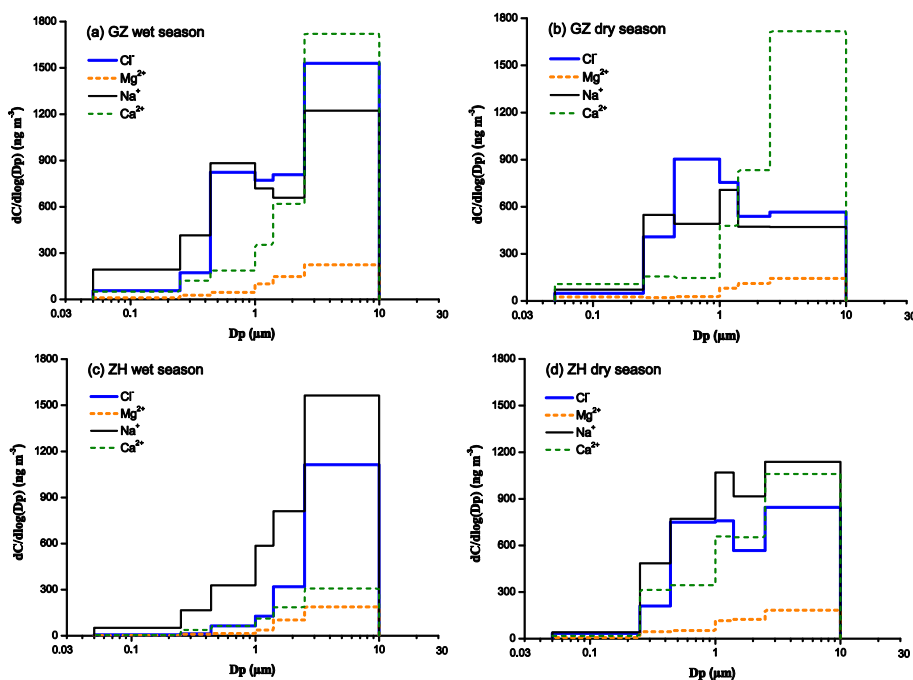


Fig. 4. Size distributions of other inorganic aerosols ( $\text{Cl}^-$ ,  $\text{Na}^+$ ,  $\text{Mg}^{2+}$  and  $\text{Ca}^{2+}$ ).

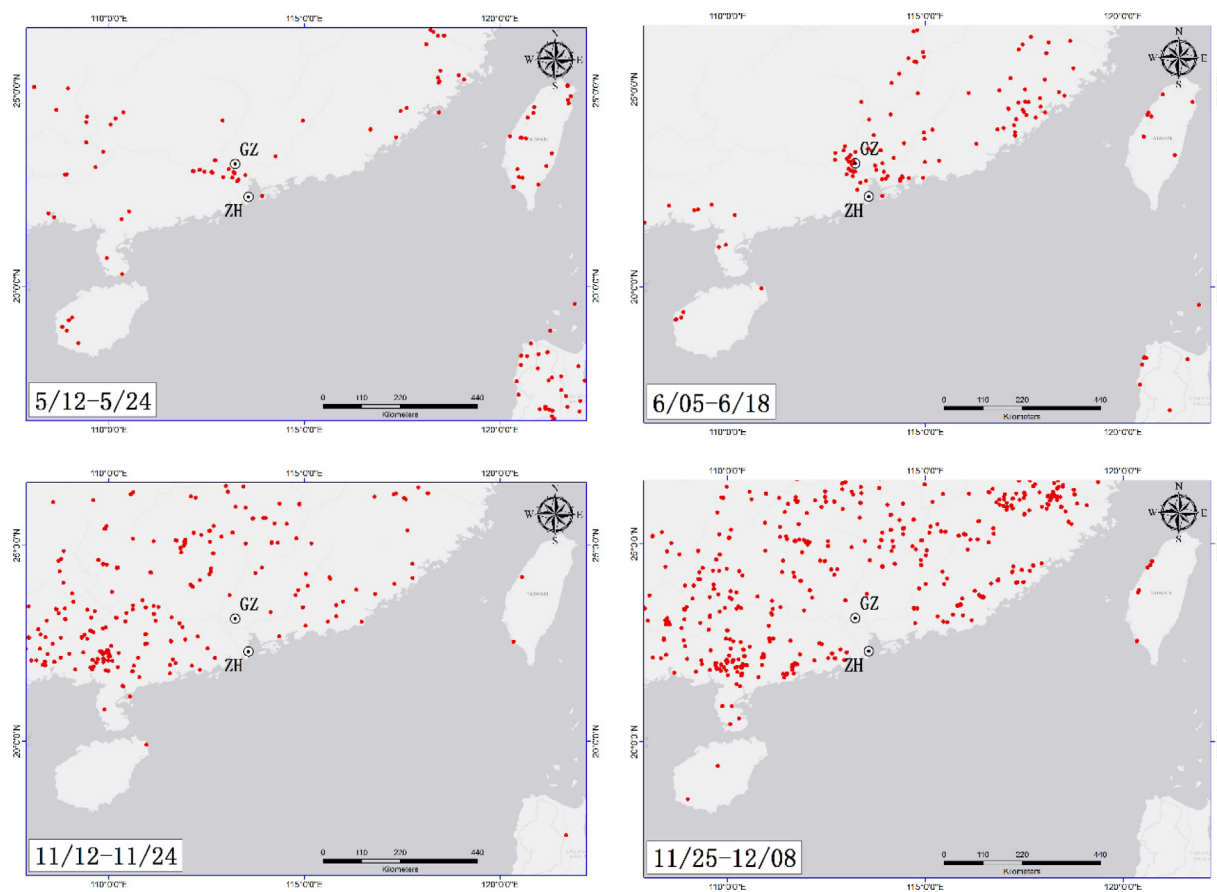


Fig. 5. MODIS fire maps for South China during the study periods.

Therefore, it is not surprising that the contributions of biomass burning emissions to the ambient aerosol burden were higher during the dry season.

Table 3 lists the biomass burning tracer levels obtained in previous studies. Clear seasonal variations of the biomass burning tracers were observed at most sites, which mainly depended on the extent of biomass burning activities. More specifically, LG levels were generally higher in the cold season than those in the warm season at many locations such as Beijing, Austria and Southeastern US (Cheng et al., 2013; Caseiro et al., 2009; Zhang et al., 2010a). As suggested in previous studies, this may be due to the extensive use of biofuels for heating in the cold season. On the other hand, LG concentrations during the dry season in the PRD region were comparable to those measured in the Southeastern US and Austria in the cold season. However, their levels were considerably lower than the values obtained at the urban Beijing site and in the Chiang Mai basin of Thailand during biomass burning episodic periods. This indicates the non-negligible impact of biomass burning on air quality in Asia.

### 3.3. Aerosol origin identification using multi-tracer relationships

The correlation and ratio between specific source tracers are useful in identifying the origins and formation processes of atmospheric aerosols. Knowledge of sources of fine particles generated from various biomass burning chamber or near-source studies from the literature were used to explain the data obtained in the present study. Scatter plots of LG versus MN and  $nss-K^+$  versus LG in  $PM_{2.5}$  are presented in Fig. 7. Since anhydrosugars are the pyrolysis

products of cellulose and hemicellulose, it is not surprising that there were significant correlations between LG and MN at both sampling sites. The regression slopes ( $\Delta LG/\Delta MN$ ) were 15.3 and 18.5 for the urban and suburban site, respectively.

The LG to MN ratio has been proposed to identify particular wood types in ambient biomass burning aerosols (Engling et al., 2009; Schmidl et al., 2008). An overview of biomass burning tracer ratios derived from various source profiles is provided in Table 4. In general, low LG/MN ratios (typically 3–7) are generated by softwood combustion. In contrast, burning of hardwoods and crop residues is typically associated with higher LG/MN ratios with a rather broad range of 10–83. Similar characteristics were also observed from the burning experiments of typical biofuels in South China. It is well documented that LG is the main product of pyrolysis from glucose units in cellulose or hemicellulose, while MN is derived from the thermal degradation of mannose in hemicellulose. Thus, LG/MN ratios are highly related to the relative content of glucose to mannose in the original (un-burned) biomass. Since softwoods contain a higher proportion of mannose units than hardwoods (Telmo and Lousada, 2011), it is therefore not surprising that lower LG/MN ratios are derived from softwoods combustion. The high  $\Delta LG/\Delta MN$  values observed in the PRD region fell into the LG/MN range produced by hardwood and crop residue burning, implying limited contributions of softwood combustion to biomass burning aerosols. This is consistent with the fact that broad-leaf trees are dominant in South China, whereas softwood species typically grow in cooler climate zones.

On the other hand,  $nss-K^+$  in  $PM_{2.5}$  correlated significantly with LG at both sites with the regression slopes ( $\Delta nss-K^+/\Delta LG$ ) ranging

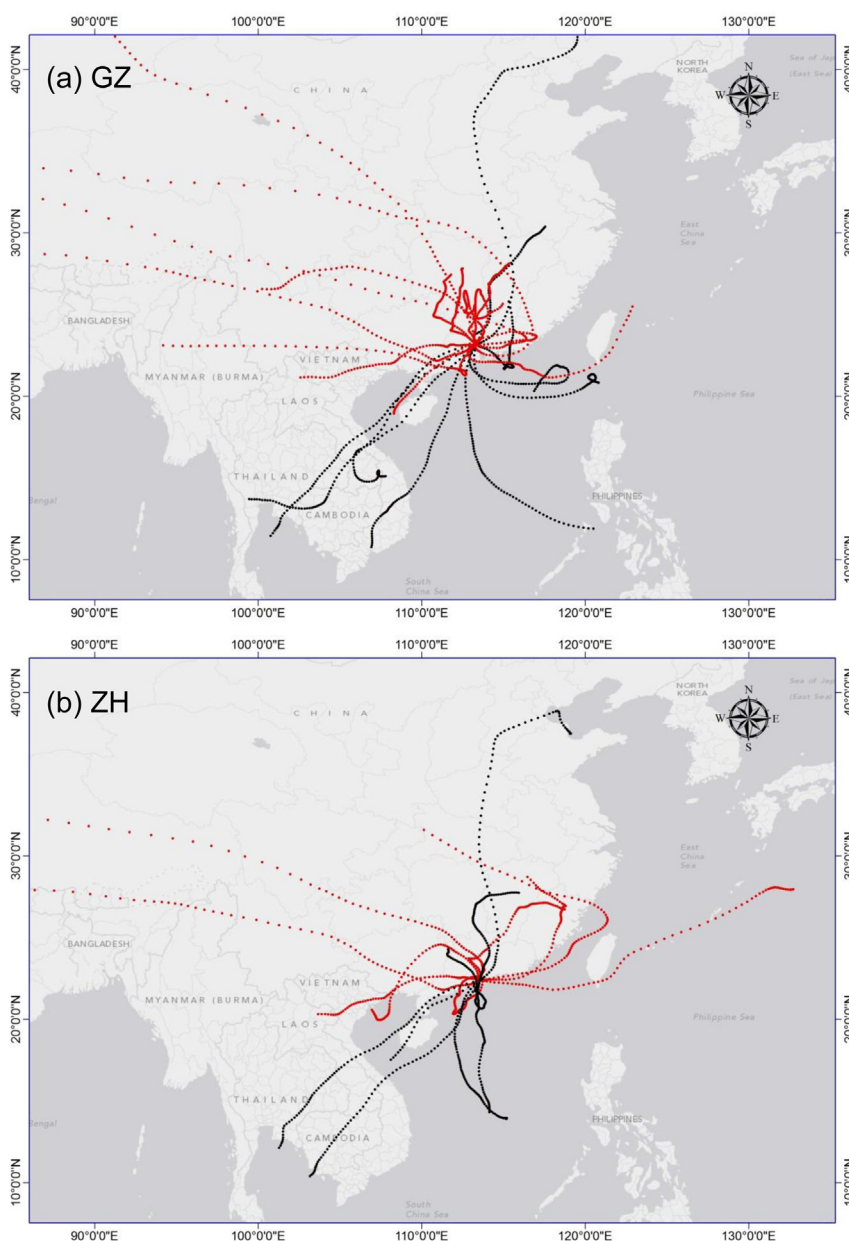


**Fig. 6.** 72 h backward trajectories (1.5 km AGL) based on HYSPLIT model for the urban (a) and suburban site (b). The black and red dotted lines represent the wet and dry season, respectively. (For interpretation of the references to colour in this figure legend, the reader is referred to the web version of this article.)

from 2.4 to 3.4 (the wet season at the suburban site is not included here). Excessive  $nss-K^+$  (large intercept) was observed for all the cases, as it is well recognized that fine-mode potassium has other potential sources such as meat grilling, vegetation and fireworks. Nevertheless, biomass burning activities were the main reason for fine potassium variation in the PRD region based on its significant correlations with LG observed in this study.

The  $nss-K^+$  to LG ratio could also be used to distinguish different biomass types or provide information about the burning conditions. The reported  $K^+/LG$  ratios ranged from 0.005 to 0.53 for softwoods grown in the USA, Austria and South China, while they ranged from 0.02 to 0.33 for hardwoods. One can easily notice that the reported ratios for hardwoods and softwoods were well below 1.0. In comparison, the  $K^+/LG$  ratios generated from crop residue burning are considerably higher than 1.0, which could be partially explained by the common use of potassium-based fertilizers in

conventional crop growing. Specifically, the  $K^+/LG$  ratios ranged from 1.4 for rice straw burning in a south Asian wood stove to 3.9 from open burning in South China, but they were lower than those for burning of wheat straw (10) and corn straw (4.8) in cooking stoves.

It should also be noted that the  $K^+/LG$  ratio is sensitive to burning conditions. According to the experiments conducted by Sullivan et al. (2008), several grass and leave burning tests gave rise to considerably high  $K^+/LG$  ratios (Table 4), while a rather broad range of  $K^+/LG$  ratios was reported (0.11–37.7). It is interesting to notice that high  $K^+/LG$  ratios were generally associated with low LG/TC ratios from burning of grasses and leaves, which might be due to LG having a higher potential to break down under high-temperature burning conditions compared to potassium. Also, Gao et al. (2003) reported that aerosols from flaming fires often have lower organic contents (normalized by potassium) compared

**Table 3**  
Biomass burning tracer levels and ratios measured in this study and other published works.

Location	Conditions	Size	LG ( $\mu\text{g m}^{-3}$ )	MN ( $\mu\text{g m}^{-3}$ )	$\text{K}^+$ ( $\mu\text{g m}^{-3}$ )	LG/MN	$\text{K}^+/\text{LG}$	References
Guangzhou, China	Wet season	$\text{PM}_{2.5}$	$0.073 \pm 0.081$	$0.006 \pm 0.007$	$0.465 \pm 0.302$	$11.5^a$	$3.4^a$	This work
	Dry season	$\text{PM}_{2.5}$	$0.272 \pm 0.103$	$0.017 \pm 0.007$	$1.197 \pm 0.356$	$15.3^a$	$2.5^a$	
Zhuhai, China	Wet season	$\text{PM}_{2.5}$	$0.008 \pm 0.009$	L.D.	$0.168 \pm 0.099$	N.A.	N.A.	This work
	Dry season	$\text{PM}_{2.5}$	$0.181 \pm 0.124$	$0.010 \pm 0.06$	$0.844 \pm 0.325$	$18.5^a$	$2.4^a$	
Beijing, China	Summer BB episodes	$\text{PM}_{2.5}$	$0.75 \pm 0.68$	$0.03 \pm 0.04$	$5.81 \pm 2.75$	25.0	9.1	Cheng et al. (2013)
	Typical Summer	$\text{PM}_{2.5}$	$0.12 \pm 0.05$	$0.01 \pm 0.00$	$0.84 \pm 0.58$	12.0	7.0	
	Typical winter	$\text{PM}_{2.5}$	$0.64 \pm 0.45$	$0.07 \pm 0.05$	$6.03 \pm 11.1$	9.0	2.0	
Urban, Chiang Mai, Thailand	Non-episodic periods	$\text{PM}_{10}$	$0.333 \pm 0.174$	$0.058 \pm 0.020$	$0.89 \pm 0.57$	5.7	2.7	Tsai et al. (2013)
	Episodic pollution	$\text{PM}_{10}$	$1.176 \pm 0.791$	$0.083 \pm 0.021$	$2.71 \pm 0.79$	14.1	2.0	
Industrial, Chiang Mai, Thailand	Non-episodic periods	$\text{PM}_{10}$	$0.413 \pm 0.254$	$0.054 \pm 0.022$	$0.83 \pm 0.45$	7.7	2.0	Tsai et al. (2013)
	Episodic pollution	$\text{PM}_{10}$	$1.073 \pm 0.647$	$0.072 \pm 0.023$	$2.04 \pm 0.72$	14.9	1.8	
Southeastern USA	Winter	$\text{PM}_{2.5}$	$0.170 \pm 0.180$	N.A.	$0.045 \pm 0.032$	N.A.	0.26	Zhang et al. (2010a)
	Spring	$\text{PM}_{2.5}$	$0.180 \pm 0.339$	N.A.	$0.056 \pm 0.052$	N.A.	0.31	
	Summer	$\text{PM}_{2.5}$	$0.019 \pm 0.045$	N.A.	$0.071 \pm 0.195$	N.A.	3.79	
	Fall	$\text{PM}_{2.5}$	$0.056 \pm 0.134$	N.A.	$0.043 \pm 0.046$	N.A.	0.77	
Montana, USA	High smoke period 1	$\text{PM}_{2.5}$	$3.471 \pm 1.827$	$0.747 \pm 0.261$	$0.443 \pm 0.408$	4.7	0.13	Ward et al. (2006)
	High smoke period 2	$\text{PM}_{2.5}$	$2.229 \pm 0.041$	$0.482 \pm 0.076$	$0.454 \pm 0.076$	4.6	0.20	
	Post-smoke baseline period	$\text{PM}_{2.5}$	$0.056 \pm 0.064$	N.A.	N.A.	N.A.	N.A.	
Three regions, Austria	Cold season	$\text{PM}_{10}$	0.19–0.86	0.034–0.212	N.A.	4.6–7.7	0.59–1.1	Caseiro et al. (2009)
	Warm season	$\text{PM}_{10}$	0.02–0.22	N.A.	N.A.	N.A.	1.8–4.5	

<sup>a</sup> The ratios of LG/MN and  $\text{K}^+/\text{LG}$  in this work are presented as  $\Delta\text{LG}/\Delta\text{MN}$  and  $\Delta\text{nss-K}^+/\Delta\text{LG}$  values, respectively.

to those derived from smoldering combustion. These observations clearly suggest that organic matter is subject to be oxidized more completely to form gaseous combustion products such as  $\text{CO}_2$  and  $\text{CO}$  in the flaming phase under high temperature burning condition. Thus, a higher  $\text{K}^+/\text{LG}$  ratio may indicate the predominance of flaming fires.

A significant correlation was found not only between LG and MN, but also between  $\text{nss-K}^+$  and LG when examining the combined data from both sites in the PRD region, suggesting that biomass burning aerosols in this region were likely influenced by a specific type of biomass burning activity. Rice is the dominant crop species in the PRD and surrounding regions, whereas the amount of grasses and leaves burned by farmers is negligible. Moreover, it was found that the burning of rice straw was associated with flaming phase combustion during the autumn harvest season (Zhang et al., 2013b). Considering the  $\Delta\text{nss-K}^+/\Delta\text{LG}$  was well within the range derived from crop residue burning, especially in the flaming mode, it was safe to conclude that the predominant type of biomass smoke aerosol in the PRD region was likely associated with rice straw burning.

The present and a few earlier studies in Asia show that biomass burning aerosols are consistently characterized by high LG/MN and  $\text{K}^+/\text{LG}$  ratios (See Table 3). For example, the mean ratios of LG/MN and  $\text{K}^+/\text{LG}$  were 25.0 and 9.1, respectively, during summer biomass burning episodes measured in Beijing (Cheng et al., 2013). However, these ratios both became smaller during the typical winter season when softwoods were suspected to be also used in non-negligible amounts for heating. Another recent study conducted by Tsai et al. (2013) in Thailand showed a much higher LG/MN ratio (~14) during the biomass burning episode than that (5–7) during the non-episodic period, suggesting the episodes were significantly influenced by the burning of crop residues. These studies shed additional light on the major biomass burning types affecting ambient aerosols in Asia, indicating that burning of crop residues is the key source of biomass smoke aerosols. In contrast, residential wood burning and forest fires are the dominant biomass burning types in North America and Europe, as supported by low  $\text{K}^+/\text{LG}$  ratios frequently detected in ambient aerosols. For example, when biomass burning activities were prevalent during winter and spring in the southeastern US,  $\text{K}^+$  and LG were reasonably correlated with a low  $\text{K}^+/\text{LG}$  ratios (Zhang et al., 2010a). Caseiro et al. (2009) also reported low LG/MN ratios (4.6–7.7) and low  $\text{K}^+/\text{LG}$  ratios

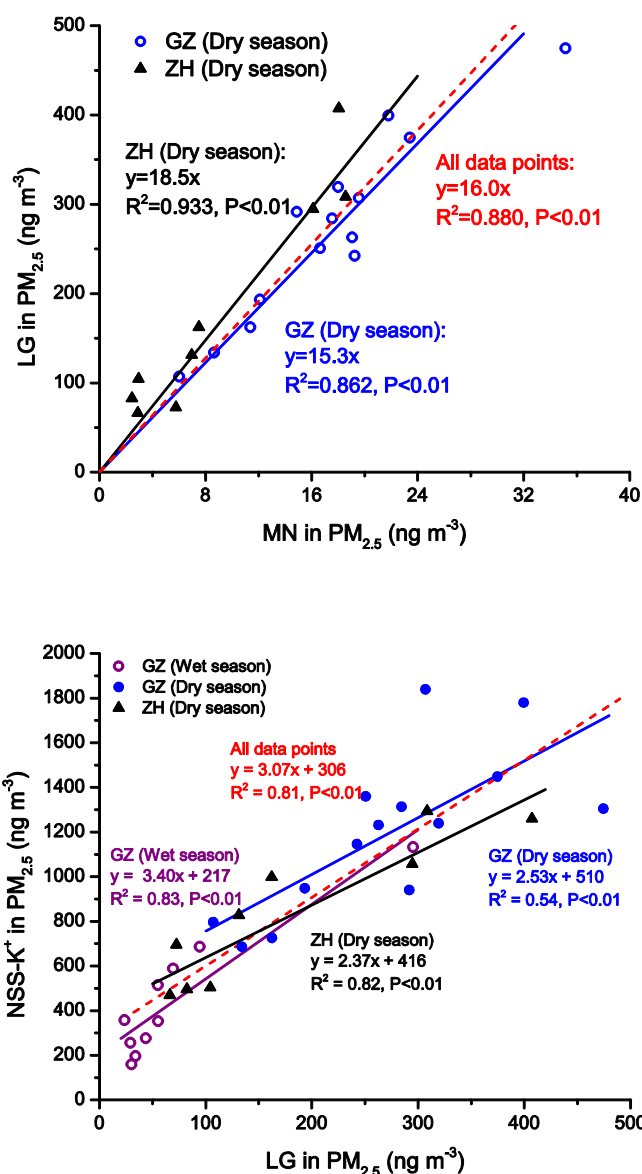


Fig. 7. Relationships between LG and MN in  $\text{PM}_{2.5}$  (upper panel), and between  $\text{nss-K}^+$  and LG (lower panel).

**Table 4**  
Overview of several critical ratios in aerosols from various biomass burning studies.<sup>a</sup>

Type	Location	Conditions	Size	LG/MN	K/LG	LG/TC	K/TC	References
13 species ( <i>Softwoods</i> )	USA	Fireplace	PM <sub>2.5</sub>	4.7 (3.4–6.7)	0.09 <sup>b</sup> (0.01–0.20)	0.10 (0.01–0.29)	0.005 (0.003–0.008)	Fine et al. (2001, 2002, 2004)
Spruce, larch ( <i>Softwoods</i> )	Austria	Wood stove	PM <sub>10</sub>	3.8 (3.6–3.9)	0.01 (0.005–0.02)	0.187 (0.14–0.23)	0.002 (0.001–0.002)	Schmidl et al. (2008)
China fir, red pine ( <i>Softwoods</i> )	China	Domestic stove	PM <sub>2.5</sub>	3.3 (3.0–3.7)	0.30 (0.07–0.53)	N.A. <sup>c</sup>	N.A.	Sang (2012)
9 species ( <i>Hardwoods</i> )	USA	Fireplace	PM <sub>2.5</sub>	25.0 (10.7–83.4)	0.08 <sup>b</sup> (0.02–0.23)	0.163 (0.08–0.34)	0.012 (0.005–0.025)	Fine et al. (2001, 2002, 2004)
Beech, oak ( <i>Hardwoods</i> )	Austria	Wood stove	PM <sub>10</sub>	14.6 (14.4–14.8)	0.04 (0.03–0.05)	0.135 (0.06–0.21)	0.005 (0.003–0.007)	Schmidl et al. (2008)
Chestnut, guger tree ( <i>Hardwoods</i> )	China	Domestic stove	PM <sub>2.5</sub>	15.9 (10.6–21.2)	0.31 (0.29–0.33)	N.A.	N.A.	Sang (2012)
Wheat, corn, rice straw ( <i>Crop residues</i> )	China	Dilution chamber	PM <sub>2.5</sub>	55.7	N.A.	0.073	N.A.	Zhang et al. (2007)
Rice straw ( <i>Crop residues</i> )	Taiwan	Open chamber	PM <sub>2.5</sub>	30.7 (12.3–55.0)	2.0 (0.8–3.4)	0.075 (0.05–0.10)	0.148 (0.072–0.337)	Sullivan et al. (2008)
Rice straw ( <i>Crop residues</i> )	Taiwan	Near source	PM <sub>2.5</sub>	26.6	2.8	0.024	0.060	Engling et al. (2009)
Rice straw ( <i>Crop residues</i> )	South Asia	Wood stove	PM <sub>2.5</sub>	41.6	1.4	0.032	0.044	Sheesley et al. (2003)
Rice straw ( <i>Crop residues</i> )	China	Domestic stove	PM <sub>2.5</sub>	16.2	2.5	N.A.	N.A.	Sang (2012)
Rice straw ( <i>Crop residues</i> )	China	Open burning	PM <sub>2.5</sub>	30.9	3.3	N.A.	N.A.	Sang (2012)
Mulberry stalks ( <i>Crop residues</i> )	China	Domestic stove	PM <sub>2.5</sub>	10.3	2.1	N.A.	N.A.	Sang (2012)
Wheat straw ( <i>Crop residues</i> )	China	Cooking stove	PM <sub>2.5</sub>	12.7	10	N.A.	N.A.	Cheng et al. (2013)
Corn straw ( <i>Crop residues</i> )	China	Cooking stove	PM <sub>2.5</sub>	19.5	4.8	N.A.	N.A.	Cheng et al. (2013)
3 kinds of duff ( <i>Biomass components</i> )	USA	Open chamber	PM <sub>2.5</sub>	1.5 (1.0–2.3)	0.08 (0.04–0.17)	0.106 (0.06–0.15)	0.007 (0.003–0.017)	Sullivan et al. (2008)
10 types of needles ( <i>Biomass components</i> )	USA	Open chamber	PM <sub>2.5</sub>	3.2 (1.4–5.4)	0.221 (0.10–0.44)	0.072 (0.03–0.13)	0.017 (0.004–0.057)	Sullivan et al. (2008)
10 types of branches ( <i>Biomass components</i> )	USA	Open chamber	PM <sub>2.5</sub>	5.2 (1.1–11.8)	0.178 (0.07–0.038)	0.084 (0.04–0.12)	0.016 (0.005–0.039)	Sullivan et al. (2008)
7 types of grasses ( <i>Biomass components</i> )	USA	Open chamber	PM <sub>2.5</sub>	18.2 (9.2–39.2)	4.8 (0.11–16.0)	0.084 (0.02–0.19)	0.166 (0.017–0.581)	Sullivan et al. (2008)
24 types of leaves ( <i>Biomass components</i> )	USA	Open chamber	PM <sub>2.5</sub>	14.5 (1.1–53.8)	5.1 (0.46–37.7)	0.043 (0.003–0.092)	0.143 (0.014–1.1)	Sullivan et al. (2008)

<sup>a</sup> Data are shown as averages, while those in brackets are the range of values.

<sup>b</sup> Potassium was reported as elemental K in this study, whereas others are water-soluble potassium.

<sup>c</sup> Hereafter, N.A. represents not available.

(0.59–1.1) for three Austrian regions during the cold season, when burning of residential wood (softwood) was prevalent.

#### 3.4. Estimation of biomass burning contributions and its implications

Several types of receptor models, such as chemical mass balance (CMB), positive matrix factorization (PMF) and simplified source-receptor approaches, have been used in source appointment studies. Due to the lack of source emission profiles in China and insufficient source indicators required by CMB and PMF models, a simplified source-receptor approach was used here to estimate the contributions from biomass burning to ambient aerosols.

This approach requires the tracers to be sufficiently stable during their atmospheric lifetime and to be emitted at a constant rate. Although LG has been considered as relatively stable in the atmosphere, it has been shown in recent lab experiments that it can potentially be oxidized by atmospheric oxidants (Hennigan et al., 2010; Hoffmann et al., 2010). Nevertheless, it is still reasonable to assume LG to be stable in the PRD region considering that (1) LG correlated significantly with potassium in the PRD region, (2) potassium is sufficiently inert in the atmosphere, and (3) both species were mainly derived from biomass burning activities in the PRD and neighboring regions where smoke particles would be transported to the monitoring sites within a short period of time during which potential LG degradation was assumed to be negligible.

Based on the overview of the conversion factors for K<sup>+</sup> or LG to TC (Table 4), the range of factors for LG was narrower, hence LG was adopted for estimation of source contributions in this study.

According to Sullivan et al. (2008), a mean value of 0.075 ( $\mu\text{g } \mu\text{gC}^{-1}$ ) was derived from Asian rice straw burning tests, and was applied here, which was very close to the values obtained from Chinese cereal straw burning (0.073) (Zhang et al., 2007). It is noteworthy that quite a small LG/TC ratio (0.024) was observed in a study of rice straw burning near the source (Engling et al., 2009). However, in this measurement rice straw was burned in the field, instead of a chamber, and smoke particles were collected downwind of the field. This burning practice had the potential to disturb underlying soil and ash particles which had high carbon contents and enhanced the carbon content of the collected aerosol particles. This was also supported by the fact that a large fraction of the total LG mass was observed in large particles ( $\text{PM} > 10$ ). Thus, we believe the emission factor of 0.075 is more representative in this region than the smaller value observed by Engling et al. (2009). Table 5 presents the statistics of the estimated TC contributions from biomass burning using this emission factor. As can be seen, elevated biomass burning TC loadings during the dry season were observed at both sites. The mean TC contributions from biomass burning were  $3.6 \mu\text{gC m}^{-3}$  and  $2.4 \mu\text{gC m}^{-3}$ , respectively, at the urban and suburban sites in the dry season, accounting for 23% and 16% of measured TC in the fine particles.

It is noteworthy that the sampling period during the dry season covered the entire period of the 16th Asian Games, which were held in Guangzhou during that year. The municipal government of Guangzhou had implemented a series of measures to reduce air pollutant levels, especially PM<sub>2.5</sub>, during the Asian Games period. More specifically, the government set “31 new rules for air cleaning” aiming to control five major pollutant sources, i.e., coal-fired

**Table 5**  
Statistics of estimated TC and contributions from biomass burning during the study period.

Site	Season	LG in PM <sub>2.5</sub> (ng m <sup>-3</sup> )			TC in PM <sub>2.5</sub> (μgC m <sup>-3</sup> )			Estimated TC from biomass burning (μgC m <sup>-3</sup> ) <sup>a</sup>			Estimated contributions of biomass burning (%)		
		Max	Min	Mean	Max	Min	Mean	Max	Min	Mean	Max	Min	Mean
Urban	Wet	295.3	23.5	73.0	23.9	6.0	10.6	3.94	0.39	0.97	16.5	4.4	7.9
	Dry	474.6	107.1	271.7	26.0	7.9	15.7	6.33	1.43	3.62	35.0	13.8	23.3
Suburb	Wet	27.1	1.9	7.5	9.8	2.4	4.5	0.36	0.02	0.10	4.7	0.4	1.9
	Dry	407.3	66.3	181.1	20.4	9.5	14.0	5.43	0.88	2.42	29.9	9.2	15.8

<sup>a</sup> TC from biomass burning is estimated using the formula:  $TC_{bb} = LG_{ambient}/Emission\ factor$ , where the emission factor used here is 0.075 (μgC m<sup>-3</sup>).

power plants, motor vehicles, fugitive dust, industrial and volatile organics emissions (Liu et al., 2013). Despite these efforts, the daily mean PM<sub>2.5</sub> mass concentration still reached up to 77.8 μg m<sup>-3</sup> (Xu et al., 2013), slightly higher than the value (75 μg m<sup>-3</sup>) of the Chinese National Ambient Air Quality Standard (NAAQS) for daily PM<sub>2.5</sub>, and more than twice of that (35 μg m<sup>-3</sup>) suggested by the NAAQS in the US. Based on the results from this study, biomass burning is a significant source for ambient TC even in urban areas, while this type of source is usually neglected by Chinese policy-makers to date. This study provides scientific evidence that it is necessary to establish biomass burning emission control policies, in particular aiming to control the open burning activities of crop residues in the PRD and other regions of China.

#### 4. Conclusions

Size-segregated biomass burning tracers were measured at an urban and a suburban site in the PRD region during a typical dry and wet season. The biomass burning origins were identified based on LG/MN and K<sup>+</sup>/LG ratios derived from combustion source profiles of several biomass groups. It was demonstrated that a multi-tracer approach is effective for identifying the specific types of burned biomass. Rather high ΔLG/ΔMN ratios were observed at both sites, indicating limited influence from softwood combustion. The high Δnss-K<sup>+</sup>/ΔLG ratios further suggested that biomass burning aerosols in the PRD region were predominately associated with the burning of crop residues.

Under the influence of intensive biomass burning activities and favored meteorological conditions, substantial enhancement of biomass smoke particles was observed during the dry season compared to the wet season. Biomass burning was identified to be a non-negligible source for fine particles in the PRD region, especially during the harvest season, with average contributions to total carbon of around 23% and 16% for the urban and suburban area, respectively, based on an LG/TC ratio of 0.075 derived from crop residue burning emissions. This study provides new insights regarding the origins of biomass smoke aerosols and their contributions to ambient aerosols and constitutes an urgently needed scientific basis for establishing effective emission control policies in areas seriously impacted by biomass burning activities.

#### Acknowledgements

We appreciate all the people who made this work possible, in particular, Shan Zhou and Qianjie Chen for providing assistance in collecting samples, and Ting Fang and Qing Ye for analyzing carbonaceous species with the carbon analyzer. This study was financially supported in part by the Special Scientific Research Funds for Environment Protection Commonweal Section (Nos. 201309011 and 201409003), National Natural Science Foundation of China (Grant Nos. 41475119 and 41375132), National Basic Research Program of China (2013FY112700), Central Research Institute's Basic Scientific Special Funds (No. PM-ZX021-201311-008),

and the Strategic Priority Research Program of the Chinese Academy of Sciences (XDB05030400).

#### Appendix A. Supplementary data

Supplementary data related to this article can be found at <http://dx.doi.org/10.1016/j.atmosenv.2014.12.009>.

#### References

- Alexander, B., Park, R.J., Jacob, D.J., Li, Q., Yantosca, R.M., Savarino, J., Lee, C., Thiemens, M., 2005. Sulfate formation in sea-salt aerosols: constraints from oxygen isotopes. *J. Geophys. Res. Atmos.* 110.
- Bond, T.C., Streets, D.G., Yarber, K.F., Nelson, S.M., Woo, J.H., Klimont, Z., 2004. A technology-based global inventory of black and organic carbon emissions from combustion. *J. Geophys. Res. Atmos.* 109 (D14).
- Cao, G., Zhang, X., Wang, Y., Zheng, F., 2008. Estimation of emissions from field burning of crop straw in China. *Chin. Sci. Bull.* 53, 784–790.
- Caseiro, A., Bauer, H., Schmidl, C., Pio, C.A., Puxbaum, H., 2009. Wood burning impact on PM<sub>10</sub> in three Austrian regions. *Atmos. Environ.* 43, 2186–2195.
- Chan, C.K., Yao, X., 2008. Air pollution in mega cities in China. *Atmos. Environ.* 42, 1–42.
- Cheng, Y., Engling, G., He, K.B., Duan, F.K., Ma, Y.L., Du, Z.Y., Liu, J.M., Zheng, M., Weber, R.J., 2013. Biomass burning contribution to Beijing aerosol. *Atmos. Chem. Phys.* 13, 7765–7781.
- Cheng, Z., Lam, K., Chan, L., Wang, T., Cheng, K., 2000. Chemical characteristics of aerosols at coastal station in Hong Kong. I. Seasonal variation of major ions, halogens and mineral dusts between 1995 and 1996. *Atmos. Environ.* 34, 2771–2783.
- Chow, J.C., Watson, J.G., Crow, D., Lowenthal, D.H., Merrifield, T., 2001. Comparison of IMPROVE and NIOSH carbon measurements. *Aerosol Sci. Technol.* 34, 23–34.
- Duan, F., Liu, X., Yu, T., Cachier, H., 2004. Identification and estimate of biomass burning contribution to the urban aerosol organic carbon concentrations in Beijing. *Atmos. Environ.* 38, 1275–1282.
- Engling, G., Lee, J.J., Tsai, Y.-W., Lung, S.-C.C., Chou, C.C.-K., Chan, C.-Y., 2009. Size-resolved anhydrosugar composition in smoke aerosol from controlled field burning of rice straw. *Aerosol Sci. Technol.* 43, 662–672.
- Fine, P.M., Cass, G.R., Simoneit, B.R., 2001. Chemical characterization of fine particle emissions from fireplace combustion of woods grown in the northeastern United States. *Environ. Sci. Technol.* 35, 2665–2675.
- Fine, P.M., Cass, G.R., Simoneit, B.R., 2002. Organic compounds in biomass smoke from residential wood combustion: emissions characterization at a continental scale. *J. Geophys. Res. Atmos.* 107.
- Fine, P.M., Cass, G.R., Simoneit, B.R., 2004. Chemical characterization of fine particle emissions from the wood stove combustion of prevalent United States tree species. *Environ. Eng. Sci.* 21, 705–721.
- Gao, S., Hegg, D.A., Hobbs, P.V., Kirchstetter, T.W., Magi, B.I., Sadilek, M., 2003. Water-soluble organic components in aerosols associated with savanna fires in southern Africa: identification, evolution, and distribution. *J. Geophys. Res.* 108, 8491.
- Harrison, R.M., Beddows, D.C.S., Hu, L., Yin, J., 2012. Comparison of methods for evaluation of wood smoke and estimation of UK ambient concentrations. *Atmos. Chem. Phys.* 12, 8271–8283.
- He, M., Zheng, J., Yin, S., Zhang, Y., 2011. Trends, temporal and spatial characteristics, and uncertainties in biomass burning emissions in the Pearl River Delta, China. *Atmos. Environ.* 45, 4051–4059.
- Hennigan, C.J., Sullivan, A.P., Collett, J.L., Robinson, A.L., 2010. Levoglucosan stability in biomass burning particles exposed to hydroxyl radicals. *Geophys. Res. Lett.* 37.
- Herckes, P., Engling, G., Kreidenweis, S.M., Collett, J.L., 2006. Particle size distributions of organic aerosol constituents during the 2002 Yosemite Aerosol Characterization Study. *Environ. Sci. Technol.* 40, 4554–4562.
- Ho, K.F., Engling, G., Ho, S.S.A., Huang, R.J., Lai, S.C., Cao, J.J., Lee, S.C., 2014. Seasonal variations of anhydrosugars in PM<sub>2.5</sub> in the Pearl River Delta region, China. *Tellus B* 66, 22577.
- Hoffmann, D., Tilgner, A., Iinuma, Y., Herrmann, H., 2010. Atmospheric stability of

- levoglucosan: a detailed laboratory and modeling study. *Environ. Sci. Technol.* 44, 694–699.
- Jimenez, J., Canagaratna, M., Donahue, N., Prevot, A., Zhang, Q., Kroll, J.H., DeCarlo, P.F., Allan, J.D., Coe, H., Ng, N., 2009. Evolution of organic aerosols in the atmosphere. *Science* 326, 1525–1529.
- Liu, H., Wang, X., Zhang, J., He, K., Wu, Y., Xu, J., 2013. Emission controls and changes in air quality in Guangzhou during the Asian Games. *Atmos. Environ.* 76, 81–93.
- Robert, J.M., Keene, W.C., Logan, J.A., Yevich, R., 1999. Global chlorine emissions from biomass burning: reactive chlorine emissions inventory. *J. Geophys. Res. Atmos.* 104, 8373–8389.
- Michalski, G., Scott, Z., Kabling, M., Thiemens, M.H., 2003. First measurements and modeling of  $\Delta^{17}\text{O}$  in atmospheric nitrate. *Geophys. Res. Lett.* 30, 1870.
- Pöschl, U., 2005. Atmospheric aerosols: composition, transformation, climate and health effects. *Angew. Chem. Int. Ed.* 44, 7520–7540.
- Sang, X.F., 2012. Carbon Isotope and Size Distributions of Biomass Burning Aerosols and Their Influence to Atmospheric Environment. Sun Yat-sen University (in Chinese).
- Schmidl, C., Marr, I.L., Caseiro, A., Kotianová, P., Berner, A., Bauer, H., Kasper-Giebl, A., Puxbaum, H., 2008. Chemical characterisation of fine particle emissions from wood stove combustion of common woods growing in mid-European Alpine regions. *Atmos. Environ.* 42, 126–141.
- Seinfeld, J.H., Pandis, S.N., 2006. *Atmospheric Chemistry and Physics: from Air Pollution to Climate Change*. Wiley-Interscience.
- Sheesley, R.J., Schauer, J.J., Chowdhury, Z., Cass, G.R., Simoneit, B.R., 2003. Characterization of organic aerosols emitted from the combustion of biomass indigenous to South Asia. *J. Geophys. Res. Atmos.* 108.
- Simoneit, B.R., 2002. Biomass burning—a review of organic tracers for smoke from incomplete combustion. *Appl. Geochem.* 17, 129–162.
- Sullivan, A., Holden, A., Patterson, L., McMeeking, G., Kreidenweis, S., Malm, W., Hao, W., Wold, C., Collett, J., 2008. A method for smoke marker measurements and its potential application for determining the contribution of biomass burning from wildfires and prescribed fires to ambient  $\text{PM}_{2.5}$  organic carbon. *J. Geophys. Res. Atmos.* 113.
- Tao, J., Shen, Z., Zhu, C., Yue, J., Cao, J., Liu, S., Zhu, L., Zhang, R., 2012. Seasonal variations and chemical characteristics of sub-micrometer particles ( $\text{PM}_{1}$ ) in Guangzhou, China. *Atmos. Res.* 118, 222–231.
- Tao, J., Zhang, L., Engling, G., Zhang, R., Yang, Y., Cao, J., Zhu, C., Wang, Q., Luo, L., 2013. Chemical composition of  $\text{PM}_{2.5}$  in an urban environment in Chengdu, China: importance of springtime dust storms and biomass burning. *Atmos. Res.* 122, 270–283.
- Tao, J., Zhang, L., Ho, K., Zhang, R., Lin, Z., Zhang, Z., Lin, M., Cao, J., Liu, S., Wang, G., 2014. Impact of  $\text{PM}_{2.5}$  chemical compositions on aerosol light scattering in Guangzhou—the largest megacity in South China. *Atmos. Res.* 135–136, 48–58.
- Telmo, C., Lousada, J., 2011. The explained variation by lignin and extractive contents on higher heating value of wood. *Biomass Bioenergy* 35, 1663–1667.
- Tian, D., Hu, Y., Wang, Y., Boylan, J.W., Zheng, M., Russell, A.G., 2008. Assessment of biomass burning emissions and their impacts on urban and regional  $\text{PM}_{2.5}$ : a Georgia case study. *Environ. Sci. Technol.* 43, 299–305.
- Tsai, Y.L., Sopajaree, K., Chotruksa, A., Wu, H.-C., Kuo, S.-C., 2013. Source indicators of biomass burning associated with inorganic salts and carboxylates in dry season ambient aerosol in Chiang Mai Basin, Thailand. *Atmos. Environ.* 78, 93–104.
- Ward, T.J., Hamilton Jr., R.F., Dixon, R.W., Paulsen, M., Simpson, C.D., 2006. Characterization and evaluation of smoke tracers in PM: results from the 2003 Montana wildfire season. *Atmos. Environ.* 36, 7005–7017.
- Xu, H.M., Tao, J., Ho, S.S.H., Ho, K.F., Cao, J.J., Li, N., Chow, J.C., Wang, G.H., Han, Y.M., Zhang, R.J., Watson, J.G., Zhang, J.Q., 2013. Characteristics of fine particulate non-polar organic compounds in Guangzhou during the 16th Asian Games: effectiveness of air pollution controls. *Atmos. Environ.* 76, 94–101.
- Zhang, L., Vet, R., Wiebe, A., Mihele, C., Sukloff, B., Chan, E., Moran, M., Iqbal, S., 2008a. Characterization of the size-segregated water-soluble inorganic ions at eight Canadian rural sites. *Atmos. Chem. Phys.* 8, 7133–7151.
- Zhang, R., Jing, J., Tao, J., Hsu, S.C., Wang, G., Cao, J., Lee, C.S.L., Zhu, L., Chen, Z., Zhao, Y., Shen, Z., 2013a. Chemical characterization and source apportionment of  $\text{PM}_{2.5}$  in Beijing: seasonal perspective. *Atmos. Chem. Phys.* 13, 7053–7074.
- Zhang, T., Claeys, M., Cachier, H., Dong, S., Wang, W., Maenhaut, W., Liu, X., 2008b. Identification and estimation of the biomass burning contribution to Beijing aerosol using levoglucosan as a molecular marker. *Atmos. Environ.* 42, 7013–7021.
- Zhang, X., Hecobian, A., Zheng, M., Frank, N., Weber, R., 2010a. Biomass burning impact on  $\text{PM}_{2.5}$  over the southeastern US during 2007: integrating chemically speciated FRM filter measurements, MODIS fire counts and PMF analysis. *Atmos. Chem. Phys.* 10, 6839–6853.
- Zhang, Y.-X., Shao, M., Zhang, Y.-H., Zeng, L.-M., He, L.-Y., Zhu, B., Wei, Y.-J., Zhu, X.-L., 2007. Source profiles of particulate organic matters emitted from cereal straw burnings. *J. Environ. Sci.* 19, 167–175.
- Zhang, Y., Shao, M., Lin, Y., Luan, S., Mao, N., Chen, W., Wang, M., 2013b. Emission inventory of carbonaceous pollutants from biomass burning in the Pearl River Delta Region, China. *Atmos. Environ.* 76, 189–199.
- Zhang, Z.-S., Engling, G., Chan, C.-Y., Yang, Y.-H., Lin, M., Shi, S., He, J., Li, Y.-D., Wang, X.-M., 2013c. Determination of isoprene-derived secondary organic aerosol tracers (2-methyltetrols) by HPAEC-PAD: results from size-resolved aerosols in a tropical rainforest. *Atmos. Environ.* 70, 468–476.
- Zhang, Z., Engling, G., Lin, C.-Y., Chou, C.C.-K., Lung, S.-C.C., Chang, S.-Y., Fan, S., Chan, C.-Y., Zhang, Y.-H., 2010b. Chemical speciation, transport and contribution of biomass burning smoke to ambient aerosol in Guangzhou, a mega city of China. *Atmos. Environ.* 44, 3187–3195.
- Zheng, J., Zhang, L., Che, W., Zheng, Z., Yin, S., 2009. A highly resolved temporal and spatial air pollutant emission inventory for the Pearl River Delta region, China and its uncertainty assessment. *Atmos. Environ.* 43, 5112–5122.
- Zheng, M., Cass, G.R., Schauer, J.J., Edgerton, E.S., 2002. Source apportionment of  $\text{PM}_{2.5}$  in the southeastern United States using solvent-extractable organic compounds as tracers. *Environ. Sci. Technol.* 36, 2361–2371.